frontiers | Frontiers in Physics

TYPE Original Research
PUBLISHED 18 December 2025
DOI 10.3389/fphy.2025.1725899

OPEN ACCESS

EDITED BY
Fei Yu,
Changsha University of Science and Technology, China

REVIEWED BY
Jingrui Liu,
Chongqing University, China
A Susi,
Pondicherry University, India

*CORRESPONDENCE
Jun Hu,
hujunwujin@gmail.com

RECEIVED 15 October 2025
REVISED 28 November 2025
ACCEPTED 30 November 2025
PUBLISHED 18 December 2025

CITATION
Li Y and Hu J (2025) Sentiment amplification and optimal control of an enhanced SEIR-based model for public opinion dissemination.
Front. Phys. 13:1725899.
doi: 10.3389/fphy.2025.1725899

Sentiment amplification and optimal control of an enhanced SEIR-based model for public opinion dissemination

YuanQing Li[1] and Jun Hu[2]*

[1]School of Cyber Science and Engineering, Southeast University, Nanjing, China, [2]School of Electronic Engineering and Optical Technology, Nanjing University of Science and Technology, Nanjing, China

In modern society, the diversification of communication channels and the multiplicity of involved actors necessitate evolving opinion propagation models from traditional single-outbreak frameworks to complex models capable of capturing multiple outbreaks. Traditional epidemic models, while widely used, fail to account for the non-linear evolution of transmission rates across different channels, overlook multiple transitions in individuals' immunity states, and neglect the influence of public attitudes on propagation dynamics. This paper proposes a systemic analysis of an enhanced public opinion propagation model and its corresponding adjoint model. Building upon the Susceptible–Exposed–Infectious–Recovered framework, the model captures four states in opinion propagation: susceptible, exposed, infected, and recovered. Two key mechanisms are introduced: transmission rates influenced by public attitudes, reflecting how attitudes modulate propagation intensity; and time-dependent immunity decay, characterizing the impact of sustained multi-channel propagation. The adjoint model quantifies opportunity costs of opinion control, providing foundations for optimal control strategies. We apply this model to a hypothetical incident simplified from a food safety public opinion event from June 2025. Through theoretical analysis and numerical simulations, we demonstrate that public attitudes significantly amplify opinion propagation, affecting both outbreak timing and scale. As the coupling strength between public sentiment and message diffusion, immunity decay, and other parameters vary, the proposed model maintains multi-stage diffusion characteristics to validate parameter settings while exhibiting adjustable peak values and timings. Compared to traditional models, information diffusion peaks increase by 32%, and peak arrival times are delayed by 17.7%. Simulation results indicate that the public attitude amplification factor serves as a critical control node—its enhancement substantially advances peak arrival time and amplifies peak intensity. The proposed model advances understanding of how public attitudes promote opinion propagation in complex social systems, and it can be extended into an interpretable neural network architecture to circumvent the black-box nature of data-driven approaches, enhancing generalization capabilities in complex network environments.

KEYWORDS

emotion coupling, information diffusion, public opinion propagation, SEIR mode, shadow price

1 Introduction

Social media has fundamentally transformed public opinion dynamics, enabling rapid information spread and emotional polarization. These platforms produce complex propagation patterns with significant societal impacts. The 2025 food-contamination incident exemplifies this transformation, evolving from localized concern to nationwide discourse through distinct emotional phases: initial shock, skepticism, sustained anxiety, and eventual recovery [1]. This case highlights the dynamic coupling between public attitudes and opinion propagation, underscoring the need for models that integrate sentiment feedback with propagation mechanisms.

Current research follows two complementary approaches. Data-driven methods learn empirical regularities from large-scale data, covering sentiment analysis and misinformation detection [2,3, 39,40], network diffusion [4,5], agent-based simulations [6,7], and other prediction methods [8,9]. Recent work includes GNN-based predictive integration [10]; models for misinformation, attribution, and missing-data bias [11–13]. Besides, researchers also developed social-physics frameworks for clarifying taxonomies [14] and neuromorphic Hopfield implementations for secure applications [15]. While powerful, these methods often trade off interpretability and direct decision support. Mechanistic approaches adapt epidemic-style frameworks to yield interpretable dynamics and intervention design. Foundational models [16,17] have been tailored to opinion propagation [18], with numerous SEIR/SIR variants. They include SI1I2R and SEI2R1R2 with media intervention and multilayer SEIR [19–21, 41], and multilingual SEIR [22]. They are also extended to co-evolving multiplex dynamics [23] and formulated as optimization problems [24,25], among others [26,27]. Further refinements include time delays [28], communication-factor coupling [29], and dynamic networks [30]. Control formulations span resource allocation [31], evolutionary games [32], and reinforcement learning [33]. Related management and sustainability studies propose the POMM opinion management model [34]; identify channels and factors shaping public p Ref. [35]; and examine corporate resilience with transmission mechanisms via green economies [36].

However, few models fully integrate the link between information and sentiment or account for sentiment-driven amplification. Current work does not provide a single view that connects changing network structure, behavior, and opinion change to decisions. In particular, traditional methods struggle to capture together time variation, network complexity, and node influence [10]. In addition, network-game models focus on behavior change, while opinion-dynamics models focus on belief change; their interaction is rarely modeled [34]. Finally, we also need clearer links from public beliefs, preferences, and behaviors to policy [36]. To address these limitations, we propose a systemic analysis of an enhanced SEIR model for public opinion propagation [18] with an associated cost evaluation model. The model tracks four opinion states and incorporates two key innovations: attitude-dependent transmission rates that reflect how public sentiment influences propagation intensity, and time-decaying immunity to capture re-exposure effects in multi-path propagation environments. The cost evaluation model computes the marginal costs of opinion evolution, enabling optimal intervention timing and in-tensity decisions. This integrated approach allows for time-varying transmission rates responsive to collective emotional states, explicit immunity waning with possible re-entry, and cost-efficient intervention strategies.

We calibrate and evaluate the model through a scenario-based reconstruction (data anonymization) of the 2025 food-contamination incident, showcasing both its explanatory accuracy and practical utility for decision-making. This study offers three primary contributions: 1. We introduce an enhanced opinion propagation model that accounts for intertwined opinion-attitude dynamics and recurring outbreak cycles. 2. We incorporate attitude-dependent transmission rates and time-decaying immunity into the SEIR framework. 3. We establish an optimal control framework grounded in cost evaluation to guide intervention timing and resource allocation strategies.

2 Theoretical framework and closed forms

The traditional Susceptible–Exposed–Infectious–Recovered (SEIR) framework, adapted from infectious disease modeling, is widely applied to simulate online public opinion diffusion. It groups users into four dynamic states and describes their evolution with ordinary differential equations. Instead of fine-grained network dispersion using spatial partial differential equations, it represents macro transmission intensity just employing a bilinear coupling between the susceptible (S) and active spreaders. Increases in the infectious (I) are buffered by the latent compartment: exposure first accumulates in the exposed (E) and is released in a constant speed of activation rate, capturing delayed activation and sensitivity to content. Simultaneously, message salience of the individual decays in another speed of recovery rate through a linear attenuation process applied to I, representing natural loss of collective attention. Remaining individuals are continually classified as still unexposed or exposed but unwilling to relay further. Thus: S comprises users not yet reached but liable to convert; E comprises users who have received the message but not acted; I comprises users actively forwarding, reposting, or endorsing; R comprises users no longer interested or unwilling to forward again.

2.1 Theoretical framework based on differential equation systems

The enhanced SEIR model conceptualizes the dissemination as a more complex system involving coupled opinion-attitude dynamics. This model extends the traditional framework by incorporating attitude-dependent transmission rates to reflect how public sentiment influences information diffusion, and time-decaying immunity to capture re-exposure effects in multipath propagation environments. Besides, the enhanced SEIR model extends the traditional framework by adding an immunity attenuation mechanism, modeling public opinion dissemination as a cyclic process. The transitions among these states form a cyclic process (S→E→I→R→S), governed by the following rates: the transmission rate $\boldsymbol{\beta(t,\ x)}$ dynamically controlling the transition from the susceptible to the exposed, the activation rate $\boldsymbol{\alpha}$ for the transition from the exposed to the infectious, the recovery rate

TABLE 1 Parameter list of the baseline transmission term.

Symbol	Meaning	Interpretation
β_{baseline}	Baseline transmission	Fundamental intensity of public opinion
δ_{decay}	Decay rate	Natural decay rate of public attention
A_i	Amplitude	Impact strength of sudden events
μ_i	Peak time	Time of sudden event occurrence
σ_i^2	Variance	Duration of public opinion shock

$\boldsymbol{\gamma}$ for the transition from the infectious to the recovered, and the immunity-decay rate $\boldsymbol{\delta}_{\text{immune}}$ for the transition from the recovered back to the susceptible. These rates respond to the emotion-driven infection process, the shift from observers to the active participants, the natural loss of interest in dissemination, and waning immunity and re-susceptibility, respectively. They are integrated into the differential Equation 1, capturing time-varying dynamics.

$$\begin{cases} \frac{dS}{dt} = -\beta(t,x)\frac{SI}{N} + \delta_{\text{immune}}R - u_1(t)S \\ \frac{dE}{dt} = \beta(t,x)\frac{SI}{N} - \alpha E \\ \frac{dI}{dt} = \alpha E - \gamma I - u_2(t)I \\ \frac{dR}{dt} = \gamma I - \delta_{\text{immune}}R + u_1(t)S + u_2(t)I \end{cases} \tag{1}$$

with initial values as Equation 2:

$$S(0) = S_0, E(0) = E_0, I(0) = I_0, R(0) = R_0 \tag{2}$$

and its boundary condition Equation 3

$$S(\text{t}) + E(\text{t}) + I(\text{t}) + R(\text{t}) = N, \text{for all } t \geq 0 \tag{3}$$

The immunity decay part is a simple linear term on the recovered group. The parameter $\boldsymbol{\delta}_{\text{immune}}$ controls how fast recovered users lose resistance; a larger value means a shorter protected period. Unlike the basic model, β(t, x) in Equation 4 is a dynamic amplification of a baseline transmission term.

$$\beta(t,x) = \beta_0(t) \cdot \left(1 - k_\beta x\right) \tag{4}$$

$$\beta_0(t) = \beta_{\text{baseline}} \exp\left(-\delta_{\text{decay}} t\right) + \sum_{i=1}^{n} A_i \exp\left(-\frac{(t-\mu_i)^2}{2\sigma_i^2}\right) \tag{5}$$

As in Equation 1, an emotion gain k_β multiplies the baseline. Stronger negative public emotion increases the gain and speeds diffusion. As in Equation 5, the baseline transmission term is an exponential decay plus weighted Gaussian peaks. The exponential decay models short-lived efficiency of message exchange. Each Gaussian peak (A_i, μ_i, σ_i^2) represents an external shock: strength, timing, and duration. All these explanations of the parameters in dynamic amplification are listed in Table 1.

Public emotion is not constant. During the 2025 food safety incident, emotion changed in several stages as new information was released. This shows that information flow shapes collective emotion. Traditional models miss this amplification because they do not couple emotion and diffusion. We improve the enhanced SEIR model by adding an emotion evolution equation to create two-way feedback. Equation 6 is a first-order linear decay on a normalized emotion index.

$$\frac{dx}{dt} = -\left(\eta_I \frac{I}{N} + \eta_E \frac{E}{N}\right)x + \left(\eta_I \frac{I}{N} x_I + \eta_E \frac{E}{N} x_E\right) + u_3(t) \tag{6}$$

with its initial value in Equation 7

$$x(0) = x_0 \tag{7}$$

It also includes the influence of spreaders and exposed users. When these two groups grow, negative emotion spreads more easily, decays more slowly, and polarization risk increases. The equation is the sum of two bilinear terms with fusion weights. These weights set the relative impact; spreaders usually have a higher weight than exposed users. Normalized emotion means the difference between public emotion and the average opinion of each group after alignment. Total population size is added; a larger population tends to stabilize emotion.

To study interventions on diffusion and emotion, we add external control inputs. Besides the control term in the baseline transmission (2.3), we include linear control terms in the equations for the susceptible, the spreader, and the emotion. Control on the susceptible means early guidance to reduce future activation. Control on spreaders means clarification and refutation to reduce active forwarding. Control on emotion means calming measures to lower collective tension.

The enhanced SEIR opinion propagation model is a high-dimensional coupled dynamical system. It requires a complete set of initial conditions as input and produces time trajectories of the state variables as output. Because of its nonlinear feedback structure, we rely on iterative numerical solvers. Beyond generating trajectories, we must analyze the simulated evolution to extract interpretable diffusion patterns. The large number of parameters further necessitates systematic sensitivity and importance assessment to guide targeted intervention design. Its parameters of the above model can be categorized into four types: system features (basic environment, e.g., total population N and time t), transmission features (dynamic diffusion, e.g., baseline β_{baseline}, emotional coupling k_β, activation α, recovery γ, and immunity decay $\boldsymbol{\delta}_{\text{immune}}$), opinion features (attitude tendencies, e.g., average opinion x(t), influence coefficients η_I and η_E, group opinions x_I and x_E), and control parameters (interventions, e.g., positive control u_1, negative handling u_2, and guidance u_3). For detailed symbols, refer to Table 2.

2.2 Closed forms based on integral equations and other comprehensive evaluations

To gain deeper insights into the mathematical properties of the model, the system can be represented in closed forms based on integral equations and in the second-order differential equations. The closed forms of the exposed population E and the infectious

TABLE 2 Critical parameters of the enhanced SEIR-Model.

Parameter	Value	Meaning
k_β	0.9	Emotions amplify dissemination
α	0.5	50% of the exposed become infectious within 1 day
γ	0.1	Individuals lose interest in dissemination after 10 days
δ	0.05	5% of the recovered return to susceptible state per day
N	1000	Base number of active internet users
β_0	0.3	Neutral dissemination capacity
η_I	0.8	Sustained influence of the infected
η_E	0.3	Sustained influence of the exposed
x_I	−0.5	Represents stance among the infected
x_E	−0.3	Represents stance among the exposed
Baseline	0.3	Fundamental intensity
Decay rate	0.05	Natural decay of public attention
Sudden event 1	Amplitude 1.2	First Gaussian peak's amplitude
	Mean 15.0	Timing
	Variance 4.0	Duration
Sudden event 2	Amplitude 1.5	Second Gaussian peak's amplitude
	Mean 30.0	Timing
	Variance 5.0	Duration

population I exhibit time accumulation effects and rapid decay behavior. Their integral representations are given as Equations 8, 9:

$$E(t) = E_0 e^{-\alpha t} + \int_0^t \beta \frac{SI}{N} e^{-\alpha(t-\tau)} d\tau \tag{8}$$

$$I(t) = I_0 e^{-\gamma t} + \int_0^t \alpha E e^{-\gamma(t-\tau)} d\tau \tag{9}$$

The above equation indicates that $I(t)$ is a weighted accumulation of historical values of $E(\tau)$, where the weighting factor decays exponentially over time. This reflects a local smoothing process applied to historical information. Besides closed forms, second-order differential equation of (I) could also insight multi-peak and oscillatory behavior in Equation 10:

$$\frac{d^2 I}{dt^2} + (\alpha + \gamma)\frac{dI}{dt} + \alpha\left(\gamma - \frac{\beta S}{N}\right) I = 0 \tag{10}$$

and Equation 11

$$\Delta = (\alpha - \gamma)^2 + \frac{4\alpha\beta S}{N} \tag{11}$$

This equation has two real eigenvalues, leading to oscillatory behavior in (I) when underdamped (i.e., when $\Delta < (\alpha + \gamma)^2$, potentially resulting in multi-peak effects).

To guide control strategies, the results of the equations should be evaluated involving comprehensive formulae. Quantify population distribution and emotional states using two variables: the instantaneous cost function and the Hamiltonian function (opportunity cost, via Pontryagin's maximum principle). The instantaneous cost function is as Equation 12

$$J = A_I I + A_E E + A_x x^2 + \frac{1}{2}\sum_{i=1}^{3} B_i u_i(t)^2 \tag{12}$$

where $A_I I$ is the social cost of infectious individuals; $A_E E$ is the risk cost of exposed individuals; $A_x x^2$ is the polarization cost (quadratic penalty for opinion deviation from neutrality); $\frac{1}{2} B_i {u_i}^2$ is the control cost (quadratic for increasing marginal costs). The Hamiltonian function is as Equation 13

$$H = J + \lambda_S \dot{S} + \lambda_E \dot{E} + \lambda_I \dot{I} + \lambda_R \dot{R} + \lambda_x \dot{x} \tag{13}$$

In Equation 13, variables $(\lambda_S, \lambda_E, \lambda_I, \lambda_x)$ denoting shadow prices represent marginal costs of state changes, which satisfy the adjoint as Equation 14:

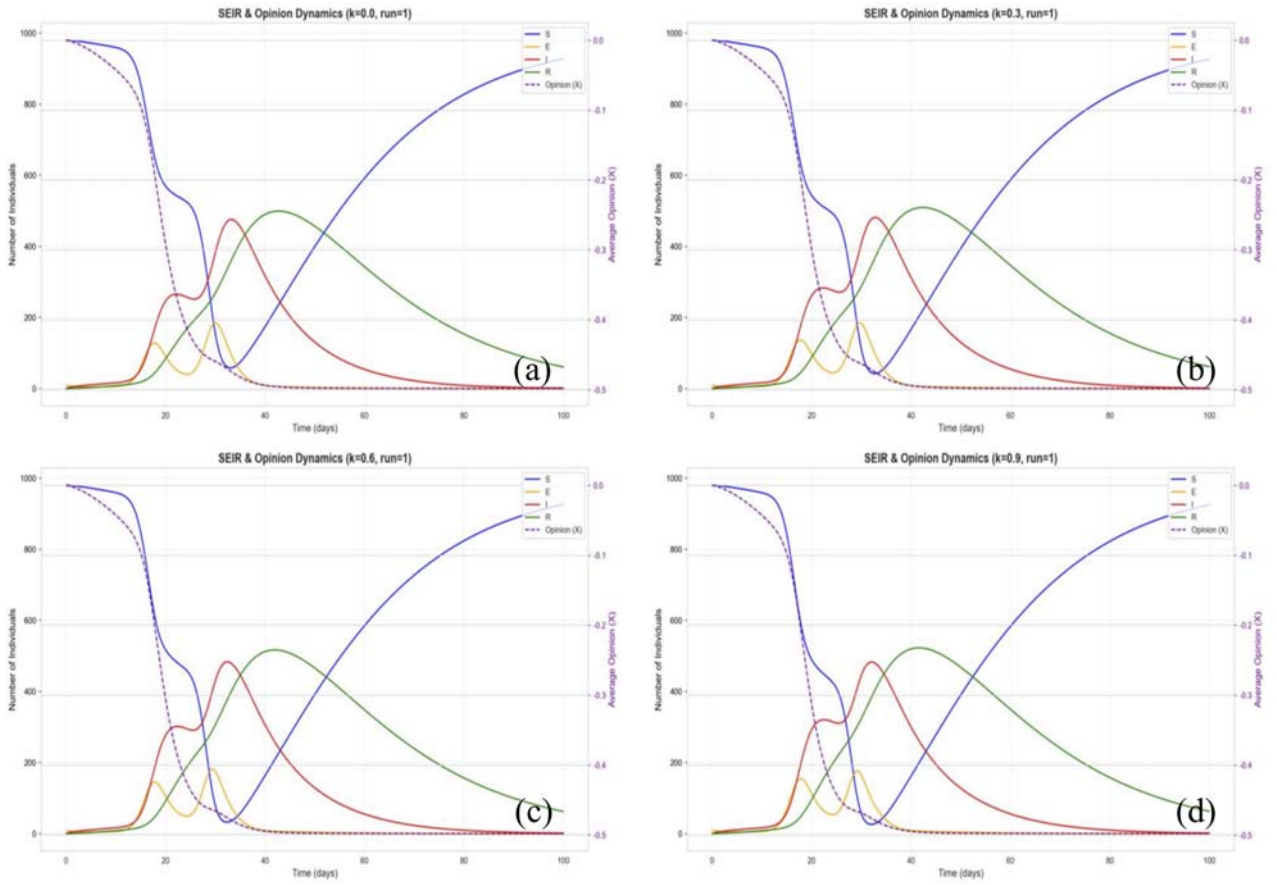

FIGURE 1
Result comparisons of different amplification factors: **(a–d)** are for 0.0, 0.3, 0.6, and 0.9, respectively.

$$\begin{cases} \dot{\lambda}_S = \beta \dfrac{I}{N}(\lambda_S - \lambda_E) + u_1(\lambda_S - \lambda_R) \\ \dot{\lambda}_E = -A_E + \alpha(\lambda_E - \lambda_I) + \eta_E \dfrac{x - x_E}{N}\lambda_x \\ \dot{\lambda}_I = -A_I + \beta \dfrac{S}{N}(\lambda_S - \lambda_E) + (\gamma + u_2)(\lambda_I - \lambda_R) + \eta_I \dfrac{x - x_I}{N}\lambda_x \\ \dot{\lambda}_R = \delta(\lambda_S - \lambda_R) \\ \dot{\lambda}_x = -2A_x x + k_\beta \beta_0 \dfrac{SI}{N}(\lambda_E - \lambda_S) + \dfrac{\lambda_x}{N}(\eta_I I + \eta_E E) \end{cases} \quad (14)$$

λ_I is the marginal cost of an additional infectious individual (typically negative, with largest absolute value). λ_x is the marginal cost of opinion deviation from public attitudes. Economically, large ($|\lambda_I|$) signals high benefit from control (u_2), guiding optimal timing and intensity.

3 Simulation and validation

In this section, we reconstruct the "2025 Food-Contamination Public Opinion Incident" to analyze its escalation stages. On 1 July 2025, the Market Supervision Bureau and Public Security Bureau of Tianshui City, investigated the Beishi Peixin Kindergarten for illegal use of food additives that caused abnormal blood lead levels in some children [37]. Following the incident, local authorities established a joint working group to conduct investigations, initiated criminal proceedings against the kindergarten's director, and pledged to hold accountable the departments responsible for regulatory failures.

3.1 A quantitative review of the event

We analyzed the evolution of this public opinion event using the volume curve, which quantifies online attention across time. According to data from an online monitoring platform, 30,964 related posts were recorded, including 21,091 short videos and 9,563 news articles [1]. The event unfolded in four stages: incubation and outbreak, emergency response, cross-provincial escalation, and social response. Before July 1, abnormal blood lead diagnoses triggered parental concern, but the discussion volume remained below 100. From July 1 to 3, official investigations and initial briefings were launched, yet the reliance on informal verbal notifications and inadequate emergency management intensified public distrust, with volume still under 100. Between July 4 and 6, cross-provincial medical examinations revealed results up to twenty times higher than local tests, and media disclosures led to rapid amplification. Two peaks appeared at 21:00 on July 5 and 6, reaching approximately 200 and 550, dominated by short

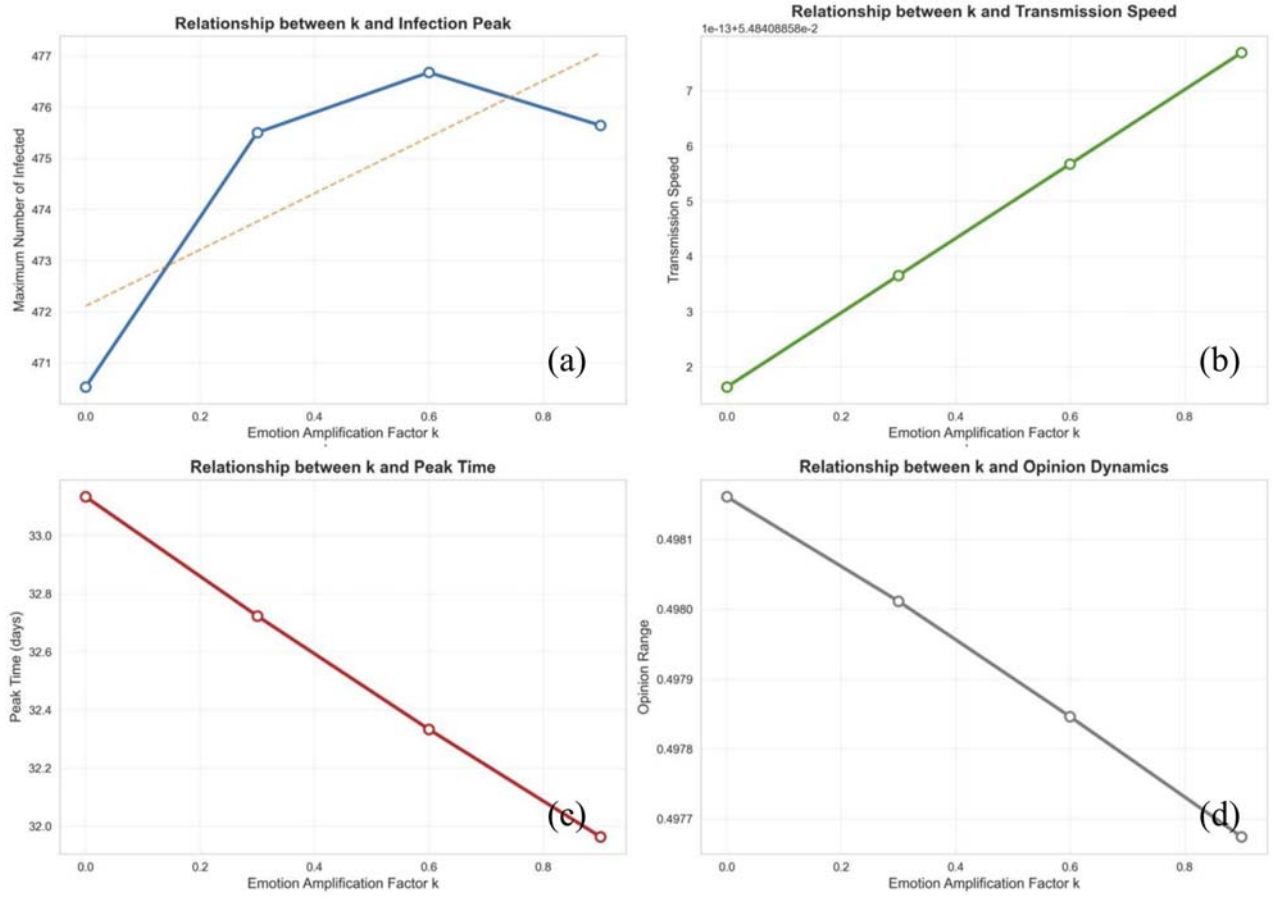

FIGURE 2
Amplification factor analysis revealing the relationship between emotional amplification and transmission dynamics. **(a)** Relationship between k and infection peak. **(b)** Relationship between k and transmission speed. **(c)** Relationship between k and peak time. **(d)** Relationship between k and opinion dynamics.

TABLE 3 Features of the infection curves against immunity decay rates.

Immunity decay rate	Infection peak (person)	Outbreak duration (Day)
0	465.40	32.11
0.02	491.46	32.44
0.05	524.21	32.44
0.08	550.41	32.78
0.1	565.08	32.78
0.15	593.87	32.78
0.2	615.26	33.11

videos. After July 7, celebrity reposts and parents' collective demands pushed the event to its climax. The peak occurred at 13:00 on July 7 with around 2,700 short videos, 700 blog posts, and 150 news articles, followed by a steep decline to about 500 by 21:00. Across all stages, short videos consistently served as the primary driver of public opinion diffusion, while news reports played a comparatively minor role.

We further assessed public sentiment using a lexicon-based approach that identifies emotional polarity by weighting sentiment, negation, and degree words [38]. Combined with dissemination

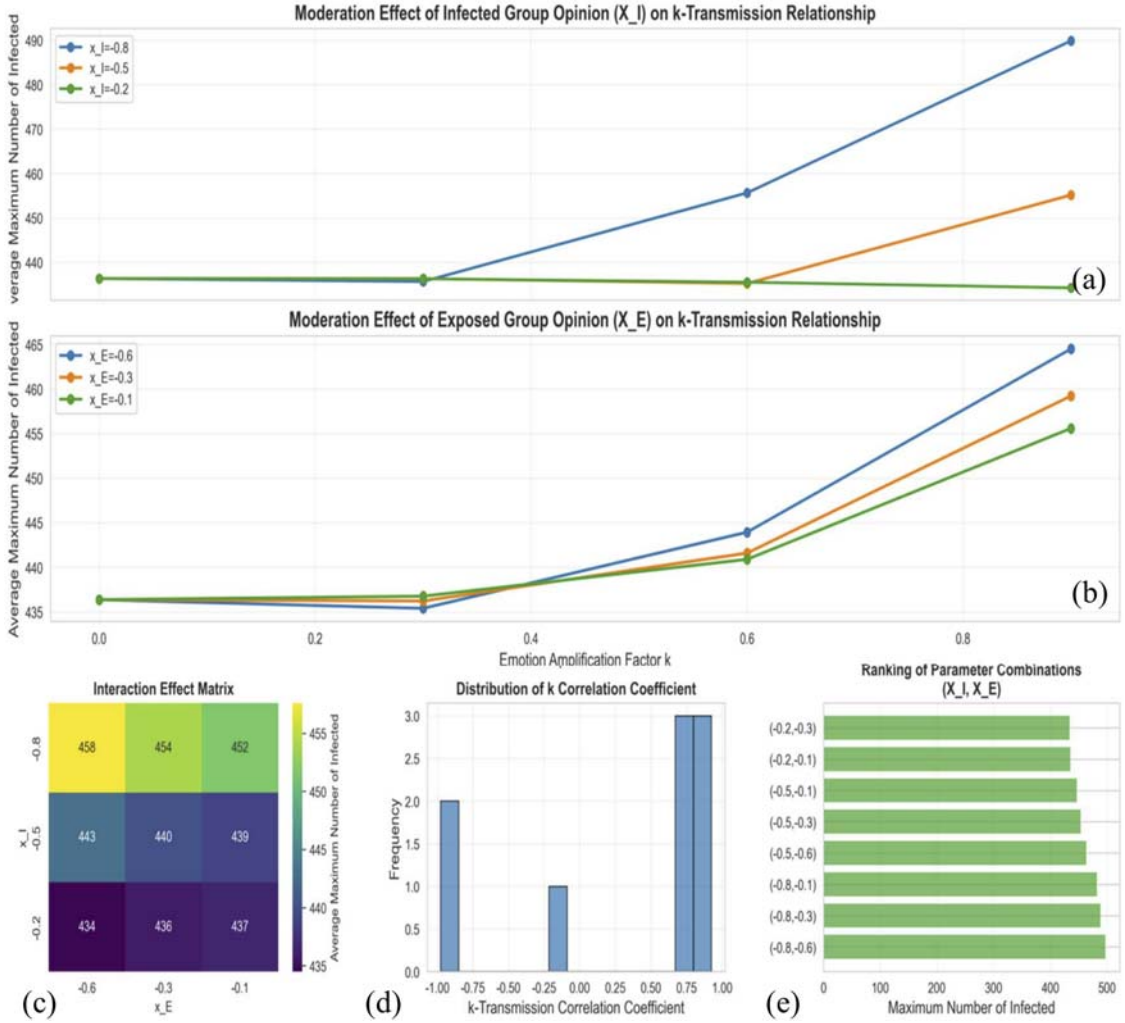

FIGURE 3
Parameter analysis of X_I and X_E. **(a)** Effect of infected group opinion on k-transmission. **(b)** Effect of exposed group opinion on k-transmission. **(c)** Interaction effect matrix of XI and XE. **(d)** Distribution of k correlation coefficient. **(e)** Ranking of parameter combinations.

TABLE 4 Features of the infection curves against amplification factors.

Amplification factor	Infection peak (person)	Peak time (Day)
0	470.53	33.13
0.3	475.50	32.72
0.6	476.68	32.33
0.9	475.64	31.96

data, the results show that negative emotions were not only dominant but also intense and highly directional. Short video platforms accounted for 51.7% of total dissemination and acted as the primary trigger of emotional resonance. Topic-specific interaction, such as the #TianshuiBloodLeadIncident hashtag reaching 1.2 million engagements, indicates the scale of negative expression. "kindergarten" (278,000 times), "blood lead" (241,000 times), and "additives" (185,000 times) reflect core public concerns. In contrast, terms such as "irreversible damage" and "intelligence decline" reveal deep-seated health anxieties. The widespread sharing of "lead-eliminating recipes" and "blood test hospital recommendation lists" further demonstrates the spread of collective anxiety among parent communities. Rule-engine sentiment scoring shows that negative emotions account for 50.7% of all

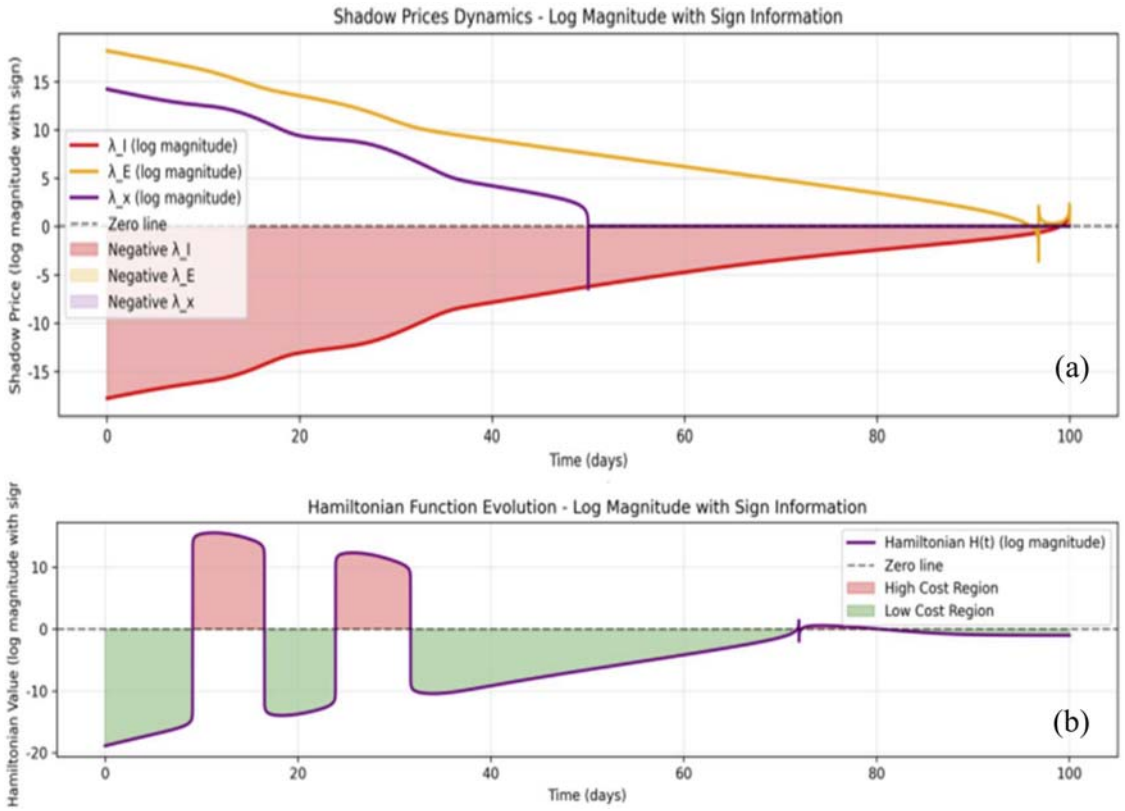

FIGURE 4
Cost analysis: **(a)** shadow price and **(b)** Hamilton function.

classified content, far exceeding positive sentiment at 3.4%. Neutral discussions at 45.9% mainly concern medical procedures and accountability issues. Overall, public sentiment exhibits a highly concentrated negative pattern, indicating a high-risk emotional environment [1].

3.2 Parameter modeling of a hypothetical simplified incident

The parameter modeling is based on a hypothetical, simplified incident model (a common practice for initial theoretical exploration).

3.2.1 Simplification and focus of the model

The primary objective of this simplification is to theoretically inform the timing and selection of control strategies for public opinion management. Consequently, our focus is placed on the peak position and morphological characteristics of the public opinion spread curve, which are then mapped to the model parameters. To simplify the system dynamics, the coupling dynamics within the emotional equation, which describes the dynamic change in public attitude, are treated under an idealized assumption.

The coupling coefficient signifies the influence of a unit number of spreaders (I) or latent individuals (S) on public sentiment. A coefficient of 0 implies no impact on public sentiment, indicating low public sensitivity to the incident. A high coefficient suggests a strong influence and high public sensitivity, making sentiment easily swayed. For this initial modeling, the coupling coefficients are assumed to lie between 0 and 1. Specifically, the influence of public opinion spreaders (I) on sentiment is hypothesized to be stronger, set at 0.8. In contrast, the influence of latent individuals (S) is assumed to be weaker, set at 0.3. These initial assumption-based values will be refined and validated using more precise parameter fitting or statistical methods as richer data become available.

3.2.2 Systematic parameter estimation

The evolution of public opinion regarding the food contamination incident follows a typical multi-stage pattern: "outbreak–intervention–decline–resurgence–resolution". Outbreak Stage: Following the initial media exposure, public opinion rapidly peaked, and negative attitudes reached their maximum intensity. Official Intervention Stage (Critical Stage): The government's launch of an investigation team corresponds to the full activation of the control variables, u_2 and u_3, within the model. This leads to a sharp decline in the infectious compartment, $I(t)$, and a rise in the recovered compartment, $R(t)$, as the dominant group. Stabilization Stage: The event enters a relatively stable state. Public opinion intensity drops significantly as public attention shifts elsewhere. Immunity Loss and Resurgence Stage (Crucial Stage): A controversial video reignited small-scale discussions. This event verifies the validity of the immunity decay mechanism $\delta R \rightarrow S$

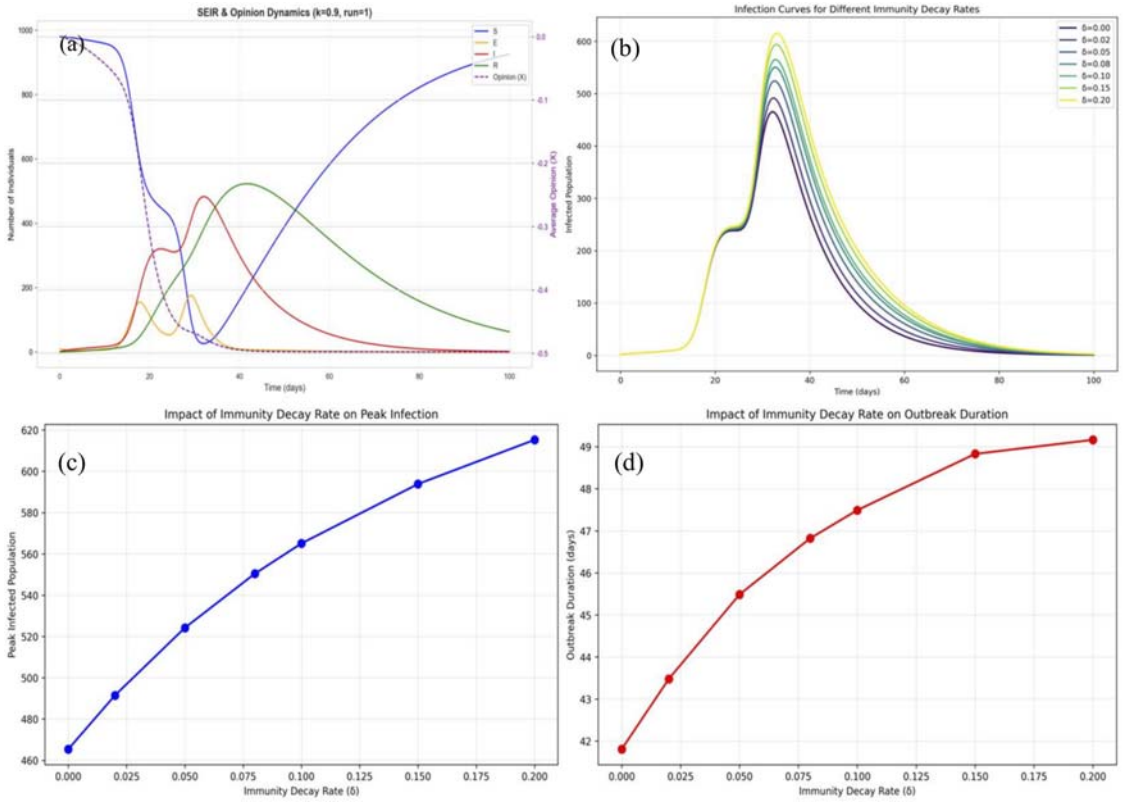

FIGURE 5
Simulation results: **(a)** dynamic results of four variables, **(b)** infection responses and their features - **(c)** the infectious peaks and **(d)** outbreak durations - against immunity delays.

in the model, where some previously "recovered" users become susceptible (S) or infectious (I) again. Final Resolution Stage: The second wave quickly dissipated, and the system returned to long-term stability.

The entire process validates the bidirectional coupling mechanism between attitudes and opinions: negative attitudes accelerate information dissemination, and the scale of dissemination further amplifies them.

Next, we will present approaches to evaluate the traditional parameters according to the timeline extracted from the above simplification. The routine is built on exponential decay or growth models. Specifying target time points and changes, it computes the dynamical parameters in a principled manner. The estimation assumes equation decoupling, simplifying the system into multiple first-order equations and employing logarithmic functions for estimation. Specifically, β_{high} -- high infection scenario, employ $I(t) = I(0)\exp\left(\beta_{\text{high}} t\right)$; β_{low} -- low infection scenario, bases on the target of doubling the number of infected individuals within 10 days; k_β -- multiplication effect parameter, calculates the attitude amplification effect via the formula $k_\beta = -1 + \beta_{\text{high}}/\beta_{\text{low}}$. Exposure conversion rate α is according to an exponential decay model $E(t) = E(0)\exp(-\alpha t)$. Recovery Rate γ and immunized decline rate are based on the targets of a 50% reduction in infected cases and recovered individuals, respectively. Principles for various parameters are presented above, while detailed estimated values are provided in Table 2. However, all these parameters should be validated and adjusted based on the simulation results to achieve a satisfactory match between the simulation and the design.

3.3 Simulation, comparisons, and other validations

We implement a coupled simulation primarily in Python. Python was chosen for its extensive ecosystem of scientific computing libraries and its readability, making it ideal for modeling complex dynamic systems. The core simulation logic analyzes waveforms and leverages a function that uses the RK45 method to numerically solve the system of Ordinary Differential Equations (ODEs) that govern the time evolution of the five state variables. The programming paradigm centers around the Waveform Simulator, which uses NumPy for numerical arrays, Pandas for structured data handling and analysis, and Matplotlib for automatic visualization of the resulting time-series waveforms and sensitivity analysis reports. The realization also follows a modular design, relying on configuration files to manage simulation parameters and control inputs, enabling systematic scenario testing and detailed parameter sensitivity studies (e.g., the immunity decay rate).

3.3.1 Model and parameter validation

We first validate the simulation model and its parameter settings. Some parameters come from a simplified reconstruction; others are

idealized assumptions. Therefore, the simulated curves keep several real-world features, especially the multi-stage pattern. Results show that with the current estimated parameters, the coupled model reproduces the expected multi-stage evolution.

The simulation reproduces five stages of opinion diffusion: fermentation, outbreak, stabilization, resurgence, and decline. Three key stages are summarized. (1) Initial Outbreak Phase: $I(t)$ rises steadily from a low base; average opinion $x(t)$ drifts from −0.1 to −0.3. The first external stimulus triggers an outbreak; infections approach 35%. Exposed (latent) individuals peak first, followed by infectious individuals. The susceptible fall and form a short plateau. (2) Public Sentiment Rebound Phase: After the plateau, a second peak appears, driven by a new stimulus and the re-entry dynamics; waning immunity amplifies this peak and splits the overall waveform. (3) Full Decline Phase: With no new stimuli, transmission weakens. Exposed declines fastest, then infectious, then recovers. The susceptibility gradually rises as immunity decays. Average sentiment settles near −0.5.

These multi-feature patterns support the plausibility of the estimated parameters and the correctness of the implementation, forming the basis for later performance discussion and sensitivity analysis.

3.3.2 Model comparison and parameter sensitivity

We compare the proposed model with two reduced versions: (a) the model without emotion coupling/amplification; (b) the model without immunity decay.

3.3.2.1 Emotion amplification analysis

The emotion amplification factor k_β represents the gain of public emotion on transmission. When $k_\beta = 0$, the model reduces to a no-emotion baseline. As k_β rises, emotion increases diffusion strength and alters peak height and timing. We examine the emotion amplification factor k_β across four regimes: $k_\beta = 0.0$ (pure rationality; transmission = β0), $k_\beta = 0.3$ (moderate influence), $k_\beta = 0.6$ (strong influence), and $k_\beta = 0.9$ (dominant emotion; rational factors suppressed). Simulations confirm that higher k_β accelerates the spread and raises the peak size while advancing peak timing. Qualitative results (Figure 1) show an unchanged basic shape but shifted maxima. Quantitative results (Figure 2) show that peak size increases with k_β; peak arrival time decreases with k_β. Table 3 shows features of the infectious curves against the amplification factors. For example, the peak infectious count rises from ~470 to ~477, and the peak time shortens from 33.1 to 31.96 days as k_β increases. The Pearson correlation between k_β and peak size is positive ($r = 0.78$); with peak timing, it is negative ($r = -1.00$). Formula:

$$r = \frac{\sum_{i=1}^{n}(x_i - \bar{x})(y_i - \bar{y})}{\sqrt{\sum_{i=1}^{n}(x_i - \bar{x})^2}\sqrt{\sum_{i=1}^{n}(y_i - \bar{y})^2}} \tag{15}$$

Here, r is the correlation coefficient; x is k_β; y is the chosen indicator. These highlight the phenomenon of "the more anger, the wider the spread."

In the analysis of positive coupling parameters, the modulatory effects of opinion parameters were also investigated. Figure 3 presents the results of the parameter sweep. The study reveals that the initial average attitudes of the infectious group (X_I) and the exposed group (X_E) have a strong regulatory effect on the influence of k_β. The most outbreak-prone combination occurs when $X_I = -0.8$ and $X_E = -0.6$, where the peak number of infectious individuals reaches 497 under $k_\beta = 0.9$. In contrast, the most stable configuration is observed when $X_I = -0.2$, where the system shows the lowest sensitivity to changes in k_β. This indicates that a hostile attitude environment intensifies the amplification effect and that pre-existing negativity creates a fertile ground for amplification. Simulation results further show that both X_I and X_E influence dissemination, but their effects are conditioned on k_β. When k_β is small, their impact is negligible—suggesting that the positive coupling effect, governed by k_β, serves as a "switch". If this switch is off, dissemination evolves independently of emotion, and emotion merely acts as a passive observer of opinion dynamics. As k_β increases, the emotional promotion of dissemination becomes significant. When k_β is sufficiently large, emotion acts as a multiplier in the spread of public opinion.

These results show "more anger, wider spread" and highlight that emotion control must combine source isolation (reducing I and E influence) with channel moderation during high emotion surges.

3.3.2.2 Immunity decay analysis

The immunity decay constant δ_{immune} measures the average time before recovered users become susceptible again. When $\delta_{immune} = 0$, there is no return; larger δ_{immune} shortens the return interval. A sensitivity test (δ_{immune} from 0.00 to 0.20) shows clearer double-peak behavior as δ increases. Table 4 shows the results of the parameter scanning, including the values of immunity decay rates and their feature responses of the infectious. The first peak reflects the original susceptible set; the second is amplified by users who lost immunity. Peak infections grow from 465 to 615 (≈32% increase), and outbreak duration extends from 41.8 to 49.2 days (≈17.7% increase). This indicates immunity loss strengthens both scale and persistence. The higher peak and shifted timing indicate that the proposed model captures resurgence more accurately than one without decay, suggesting that extending the adequate "protection time" (public guidance) lowers later amplification.

Effective public opinion management focuses on establishing long-term governance mechanisms, with attention to trade-offs between cost and intervention.

To this end, we analyzed management cost and opportunity cost. Figure 4 presents the evolution of two key auxiliary indicators. Shown in Figure 4a, the shadow price approaches zero over time, indicating that opportunity cost diminishes in the later stages of dissemination. This implies that early-stage intervention is most cost-effective. As shown in Figure 4b, the Hamiltonian function under the no-control scenario exhibits a decay trend over time, consistent with the common-sense expectation that intervention should occur early. The shadow price also reveals that the main cost driver is the infectious population, suggesting that targeting $I(t)$ through interventions (e.g., lowering the infection rate) is most effective. Furthermore, late-stage control of the average opinion $x(t)$ is ineffective, as the opportunity cost is minimal—consistent with Figure 5, which shows that $x(t)$ stabilizes in the later phase. Figure 4b also highlights the existence of high-cost and low-cost temporal zones for intervention. During the high-cost period, dominated by external stimuli, control yields little return because those stimuli are uncontrollable.

4 Conclusion

This study introduces an enhanced SEIR model that combines public attitude dynamics with opinion propagation. The model incorporates two key features: attitude-dependent transmission rates and exponential decay of immunity. Our analysis reveals that public attitudes significantly influence when and how rapidly opinions spread. The immunity decay mechanism helps explain why opinions can re-emerge over time. The model also provides insights for optimizing intervention timing and intensity. As the coupling strength, immunity decay, and other parameters vary, the proposed model maintains multi-stage diffusion characteristics while exhibiting adjustable peak values and timings. Compared to traditional models, information diffusion peaks increase by 32%, and peak arrival times are delayed by 17.7%. This framework improves our understanding of how attitudes amplify opinion propagation, supporting better monitoring and management strategies. However, the model makes simplifying assumptions about population mixing and attitude-opinion relationships that may not capture the complexities of the real world. Future work could integrate these theoretical mechanisms into deep learning models, creating hybrid approaches that maintain interpretability while improving performance in complex network environments.

Data availability statement

The authors confirm that the data supporting the findings of this study are derived from publicly available datasets, which have been acknowledged within the article.

Author contributions

YL: Conceptualization, Funding acquisition, Investigation, Methodology, Software, Visualization, Writing – original draft, Writing – review and editing. JH: Conceptualization, Data curation, Formal Analysis, Resources, Supervision, Validation, Writing – review and editing.

Funding

The author(s) declared that financial support was received for this work and/or its publication. This work is supported by the Big Data Computing Center of Southeast University.

Acknowledgements

The authors would like to thank the editor-in-chief, the editor, and the reviewers for their valuable comments and suggestions.

Conflict of interest

The author(s) declared that this work was conducted in the absence of any commercial or financial relationships that could be construed as a potential conflict of interest.

Generative AI statement

The author(s) declared that generative AI was not used in the creation of this manuscript.

Any alternative text (alt text) provided alongside figures in this article has been generated by Frontiers with the support of artificial intelligence and reasonable efforts have been made to ensure accuracy, including review by the authors wherever possible. If you identify any issues, please contact us.

Publisher's note

References

1. Dingxiang Bidding Information and Report Database. Public opinion analysis report on the abnormal blood lead incident in a tianshui, Gansu kindergarten (2025). Available online at: https://dxqxpt.com/h-nd-36980.html (Accessed 8 July 2025).

2. Tang D, Wei F, Yang N, Zhou M, Liu T, Qin B. Learning sentiment-specific word embedding for Twitter sentiment classification. In: *Proceedings of the 52nd annual meeting of the association for computational linguistics (volume 1: long papers)*. Baltimore, Maryland: Association for Computational Linguistics (2014). p. 1555–65. doi:10.3115/v1/P14-1146

3. Li Y, Dai M, Zhang S. FHGraph: a novel framework for fake news detection using graph contrastive learning and LLM. *Comput Mater Contin* (2025) 83:309–33. doi:10.32604/cmc.2025.060455

4. Hou D, Liu C, Li Y. Internet public opinion diffusion: a cross perspective of multilayer network and multisubject association. *Math Probl Eng* (2022) 2022:6087476. doi:10.1155/2022/6087476

5. Cao L, Zhao H, Wang X, An X. Competitive information propagation considering local–global prevalence on multi-layer interconnected networks. *Front Phys* (2023) 11:1293177. doi:10.3389/fphy.2023.1293177

6. Wang R, Lu T, Zhang P, Gu N. Data-driven agent-based model for public opinion propagation simulation in cyberbullying. *Big Data Min Anal* (2025) 8:794–819. doi:10.26599/BDMA.2024.9020042

7. Riazi D. *Agent-based models of social learning in opinion dynamics*. London: University College London (2025).

8. Jia C, Jiao D, Xu Z, Deng G, Li T, Wang R. A prediction model for the propagation of hot topics based on representation learning and group identity. *Expert Syst* (2025) 2025:128353. doi:10.1016/j.eswa.2025.128353

9. Noorazar H. Recent advances in opinion propagation dynamics: a 2020 survey. *Eur Phys J Plus* (2020) 135:521. doi:10.1140/epjp/s13360-020-00541-2

10. Tong Q, Xu X, Zhang J, Xu H. Public opinion propagation prediction model based on dynamic time-weighted rényi entropy and graph neural network. *Entropy* (2025) 27:516. doi:10.3390/e27050516

11. Yin Y, Chen Z, Bao X. Bidirectional temporal-delay graph convolutional network for detecting fake news. *Eng Appl Artif Intell* (2024) 133:108368. doi:10.1016/j.engappai.2024.108368

12. Liu J, Duan Z, Hu X, Zhong J, Yin Y. Detracking autoencoding conditional generative adversarial network: improved generative adversarial network method for tabular missing value imputation. *Entropy* (2024) 26:402. doi:10.3390/e26050402

13. Downing NJ. Missing value imputation in environmental, social, and governance data: an impact on emissions scores. *Finance Res Lett* (2025) 85:107818. doi:10.1016/j.frl.2025.107818

14. Paul S, Mukherjee D, Mitra A, Mitra A, Dutta PK. Unravelling the complex networks of social physics: exploring human behavior, big data, and distributed systems. *J Soc Comput* (2024) 5:165–79. doi:10.23919/JSC.2024.0014

15. Yu F, Kong X, Yao W, Zhang J, Cai S, Lin H. Dynamics analysis, synchronization and FPGA implementation of multiscroll hopfield neural networks with non-polynomial memristor. *Chaos Solitons Fractals* (2024) 179:114440. doi:10.1016/j.chaos.2023.114440

16. Diekmann O, Heesterbeek JAP, Britton T. *Mathematical tools for understanding infectious disease dynamics*. Princeton, NJ: Princeton University Press (2012).

17. Valente TW, Davis RL. Accelerating the diffusion of innovations using opinion leaders. *Ann Am Acad Polit Social Sci* (1999) 566:55–67. doi:10.1177/0002716299566001005

18. Zhang Y, Tang W, Ni T. A public opinion propagation model for technological disasters. *Sci Rep* (2025) 15:7809. doi:10.1038/s41598-025-91244-0

19. Ge Q, Huang C, Xu H, Zhang J, Wang H. A novel SIR model-based public opinion propagation and optimal control. In: *2024 china automation congress (CAC)*. Qingdao, China: IEEE (2024). p. 558–63. doi:10.1109/CAC63892.2024.10865290

20. Geng L, Zheng H, Qiao G, Geng L, Wang K. Online public opinion dissemination model and simulation under media intervention from different perspectives. *Chaos Solitons Fractals* (2023) 166:112959. doi:10.1016/j.chaos.2022.112959

21. Wang J, Guo X, Li Y, Chun L. An improved propagation model of public opinion information and its governance in online social networks under Omni-media era. Electron. *Res Arch* (2024) 32:6593–617. doi:10.3934/era.2024308

22. Dong S, Xu L, Lan Z-Z, A Y, Bu F, Hua W. Multilingual SEIR public opinion propagation model with social enhancement mechanism and cross transmission mechanisms. *Sci Rep* (2024) 14:31081. doi:10.1038/s41598-024-82024-3

23. Ma W, Zhang P, Zhao X, Xue L. The coupled dynamics of information dissemination and SEIR-based epidemic spreading in multiplex networks. *Physica A* (2022) 588:126558. doi:10.1016/j.physa.2021.126558

24. Kuhlman CJ, Anil Kumar VS, Ravi SS. Controlling opinion propagation in online networks. *Comput Netw* (2013) 57:2121–32. doi:10.1016/j.comnet.2012.11.025

25. Ali HM, Owyed S, Ameen IG. Fractional optimal control problem and stability analysis of rumor spreading model with effective strategies. *Mathematics* (2025) 13:1746. doi:10.3390/math13111746

26. Wang P, Pan FC, Huo J, Wang XM. Non-equilibrium diffusion in a particle system and the correspondence to under-standing the propagation of public opinion. *Nonlinear Dyn* (2021) 105:1121–36. doi:10.1007/s11071-021-06597-8

27. Li Q, Du YJ, Li ZY, Hu J, Hu R, Lv B. HK–SEIR model of public opinion evolution based on communication factors. *Eng Appl Artif Intell* (2021) 100:104192. doi:10.1016/j.engappai.2021.104192

28. Zhang J, Wang X, Xie Y, Wang M. Research on multi-topic network public opinion propagation model with time delay in emergencies. *Physica A* (2022) 600:127409. doi:10.1016/j.physa.2022.127409

29. Li W, Zeng F, Zhou W, Chen Z. Internet public opinion diffusion mechanism in public health emergencies: based on entropy flow analysis and dissipative structure determination. *Front Public Health* (2021) 9:731080. doi:10.3389/fpubh.2021.731080

30. Yuan J, Shi J, Wang J, Liu W. Modelling network public opinion polarization based on SIR model considering dynamic network structure. *Alex Eng J* (2022) 61:4557–71. doi:10.1016/j.aej.2021.10.014

31. Sun H, Hu R, Lv B. Platform-oriented event time allocation (extended abstract). In: 2022 IEEE 38th International Conference on Data Engineering (ICDE); 09-12 May 2022; Kuala Lumpur, Malaysia. IEEE (2022). p. 1525–36.

32. Helfmann L, Djurdjevac Conrad N, Lorenz-Spreen P, Schütte C. Modelling opinion dynamics under the impact of influencer and media strategies. *Sci Rep* (2023) 13:19375. doi:10.1038/s41598-023-46187-9

33. Adams JA, White G, Araujo RP. Person-to-person opinion dynamics: an empirical study using an online game. *PLoS ONE* (2022) 17:e0275473. doi:10.1371/journal.pone.0275473

34. Xu Y, Liu X, Yuan J, Luo J, Zhou W, Yu M. POMM: a public opinion management model integrating network game and opinion dynamics for social networks. *Knowl.-Based Syst* (2025) 310:112964. doi:10.1016/j.knosys.2025.112964

35. Hou Z, Liu J, Pang J. Green transition and climate adaptation: empirical evidence of corporate resilience in the low-carbon economy. *Glob NEST J* (2025) 27:1–22. doi:10.30955/gnj.07421

36. Gazmararian AF, Mildenberger M, Tingley D. Public opinion foundations of the clean energy transition. *Environ Polit* (2025) 1–23. doi:10.1080/09644016.2025.2508563

37. Lu C. The entangled history of lead and human civilization. *Public Sci* (2025) 39:34–7. doi:10.3969/j.issn.1006-3315.2025.39.016

38. Webb GI. Naïve bayes. In: C Sammut, GI Webb, editors. *Encyclopedia of machine learning and data mining*. Boston, MA: Springer (2017). doi:10.1007/978-1-4899-7687-1_581

39. Tang D, Qin B, Liu T. Learning semantic representations of users and products for document level sentiment classification. In: *Proceedings of the 53rd annual meeting of the association for computational linguistics and the 7th international joint conference on natural language processing (volume 1: long papers)*. Beijing, China: Association for Computational Linguistics (2015). 1014–23. doi:10.3115/v1/P15-1098

40. Tang D, Wei F, Qin B, Yang N, Liu T, Zhou M. Sentiment embeddings with applications to sentiment analysis. *IEEE Trans Knowl Data Eng* (2016) 28:496–509. doi:10.1109/TKDE.2015.2489653

41. Geng L, Yang S, Wang K, Zhou Q, Geng L. Modeling public opinion dissemination in a multilayer network with SEIR model based on real social networks. *Eng Appl Artif Intell* (2023) 125:106719. doi:10.1016/j.engappai.2023.106719